Supporting Information

Polymer Modification on NiOx Hole Transport Layer Boosts Open-Circuit Voltage to 1.19 V for Perovskite Solar Cells

Xiaomei Lian [†⊥], *Jiehuan Chen* [†⊥], *Shiqi Shan* [†], *Gang Wu* [*,†] *and Hongzheng Chen* [†]

[†]MOE Key Laboratory of Macromolecular Synthesis and Functionalization, State Key Laboratory of Silicon Materials, Department of Polymer Science and Engineering, Zhejiang University, Hangzhou 310027, P.R. China

E-mail: samy@zju.edu.cn

Experimental Section

Materials: Ethylene glycol, Bathocuproine (BCP, 99%), methylamine hydrochloride (MACl, 99%) and methylamine hydroiodide (MAI, 99%) were purchased from TCI. N-methyl pyrrolidine (NMP, 99%), chloroform (CF, 99%), isopropanol, toluene, polystyrene (PS, average M_w ~280000), poly(methyl methacrylate) (PMMA, average M_w ~350000) were bought from Sigma Aldrich. N, N-dimethylformamide (DMF, 99%), Nickel(II) nitrate hexahydrate (96%) and ethylenediamine were bought from Alfa Aesar. Poly[bis(4-phenyl)(2,4,6-trimethylphenyl)amine](PTAA, M_w:15000-25000), 2,2',7,7'-Tetrakis[N,N-di(4-methoxyphenyl)amino]-9,9'-spirobifluorene

(Spiro-OMeTAD, 99%) $PbBr_2$ (99.99%) and PbI_2 (99.99%) were bought from Xi'an p-OLED. [6, 6]-phenyl-C_{61}-butyric acid methyl ester (PCBM, 99%) was bought from American Dye Source. All materials were used without further purification.

Device fabrications and Characterizations: The indium tin oxide (ITO) coated glass substrates were cleaned sequentially in detergent, acetone isopropanol and ethanol ultrasonic bath for 15 min, respectively. After that, the substrates were dried in nitrogen flow and cleaned by UV-Ozone treatment for 20 min before use. NiOx film was prepared according to the literature report. In one word, NiOx film was spin-coated from the precursor solution containing Nickel(II) nitrate hexahydrate: ethylenediamine = 1 M: 1 M in ethylene glycol onto ITO glass and was annealed at 150 ^oC for 0.5 h and 300 ^oC for 1 h. PTAA, PMMA or PS was dissolved in toluene with a concentration of 1.0 mg/ml, and was spin coated on NiOx substrates at a speed of 4000 rpm to form the NiOx/polymer hybrid substrate, respectively. For the perovskite precursor, MAI, PbI_2, MACl and $PbBr_2$ were mixed by 0.95:0.95:0.05:0.05 molar ratio in DMF and NMP (4:1) mixture with the concentration of 1.2 M. Both these perovskite precursor solution and substrates were heated at 70 ^oC before spin coating. Then we transferred the substrate to the spin coater and dropped the hot precursor solution onto the heated substrate and start the spin coating immediately. The spin-coating process started initially at 1000 rpm for 10 s and then 6000 rpm for 30 s. At the second procedure, 50 μl toluene was dropped after around 15 s. When it stopped, we transferred the film to the hot plate and annealed it at 100 ^oC for 2 min. PCBM solution (5 mg/ml in CF) was spin-coated on perovskite at 2000 rpm for 30 s.

BCP (0.5 mg/ml in isopropanol) was then spin-coated on PCBM at 4000 rpm for 30 s, followed by deposition of 100 nm Ag in vacuum chamber under a high vacuum of 5×10^{-4} Pa.

The X-ray diffraction patterns were recorded at a scan rate of 10° min^{-1} on Shimadzu XRD-7000 X-ray diffractometer with Cu K_α radiation (0.15406 nm). The UV-Visible absorption spectra were taken on UV-2450 UV-Vis Shimadzu Spectrophotometer. The field-emission scanning electron microscope (FESEM) measurements were carried out on Hitachi S-4800 machine. The atomic force microscope (AFM) measurement was carried out on Veeco MultiMode machine with the tapping mode. Ultraviolet photoelectron spectra (UPS) was performed on AXIS Supra (Kratos), the incident light energy is 21.22 eV. The photocurrent density-voltage (J-V) measurement was performed via the solar simulator (SS-F5-3A, Enlitech) along with AM 1.5 G spectra whose intensity was calibrated by the certified standard silicon solar cell (SRC-2020, Enlitech) at 100 mV cm^{-2}. The *J-V* measurement was performed in glovebox under N_2 atmosphere without a shade mask, and the device area is 0.115 cm^2, which is defined by the cross section of Ag and ITO. The voltage step is 0.02 V, with a delay time of 10 ms $step^{-1}$, the total scanning rate is 0.095 V s^{-1}. The external quantum efficiency (EQE) data were obtained by using the solar-cell spectral-response measurement system (QE-R, Enlitech). The dark *J-V* curve was measured by Keithley source 4200.

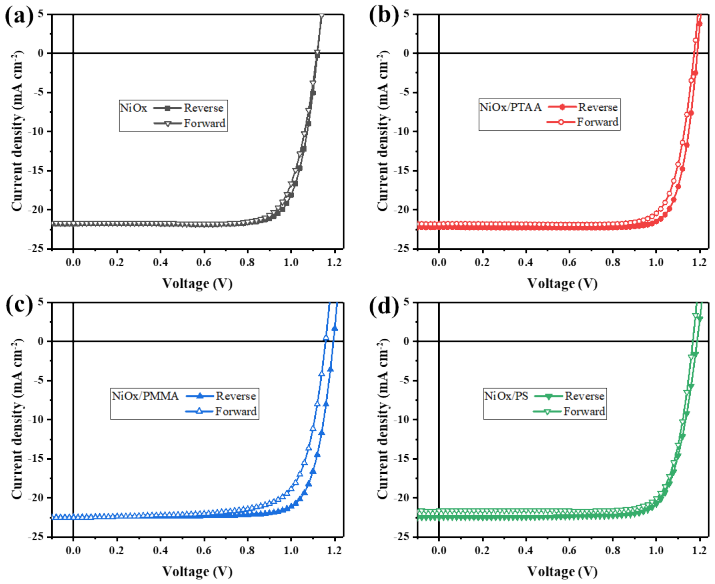

Figure S1. Forward-reverse *J-V* curves of the PVSCs with NiOx (a), NiOx/PTAA (b), NiOx/PMMA (c), and NiOx/PS (d) under 1 sun illumination (100 mW cm^{-2}).

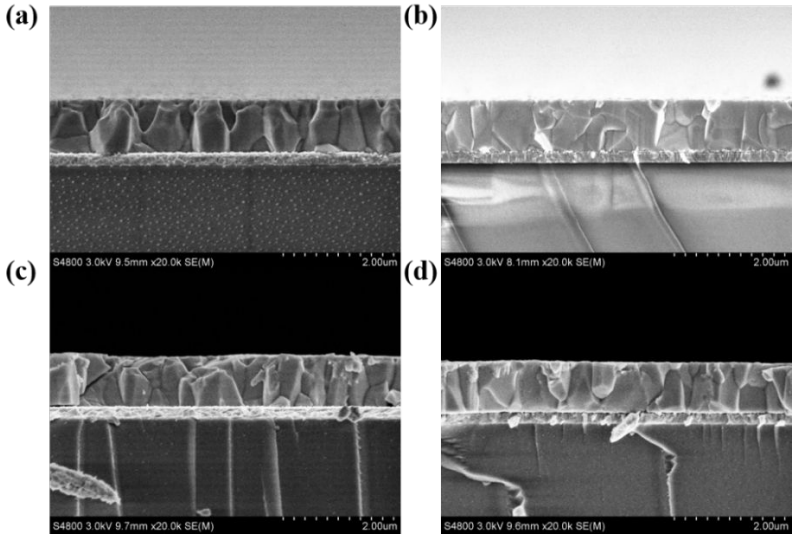

Figure S2. Top SEM images of perovskite films grown on NiOx (a), NiOx/PTAA (b), NiOx/PMMA (c), and NiOx/PS (d).

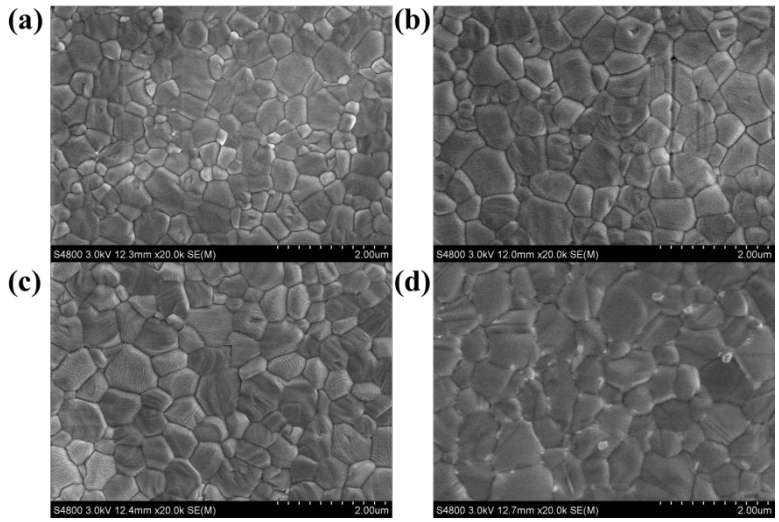

Figure S3. Top SEM images of perovskite films grown on NiOx (a), NiOx/PTAA (b), NiOx/PMMA (c), and NiOx/PS (d).

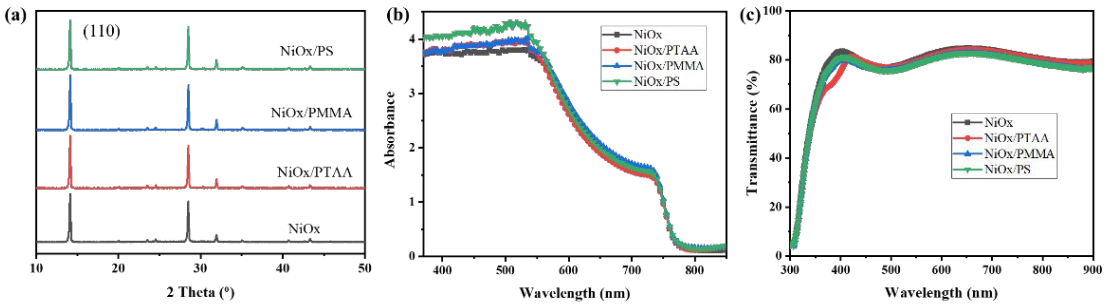

Figure S4. XRD patterns (a) and UV-Vis absorption spectra (b) for the perovskite films deposited on different substrates. (c) Transmittance spectra of NiOx with and without polymer modification on ITO glasses.

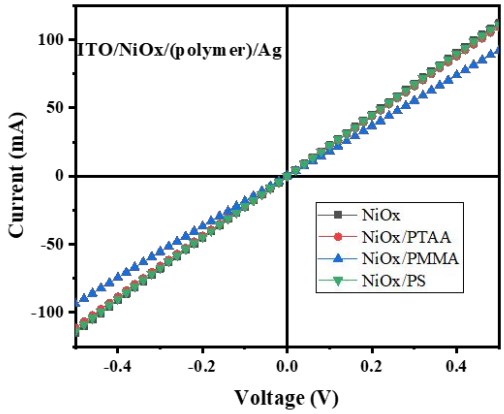

Figure S5. The conductivity measurement for different substrates with a device structure of ITO/ NiOx (w/ or w/o polymer interface layer)/Ag.

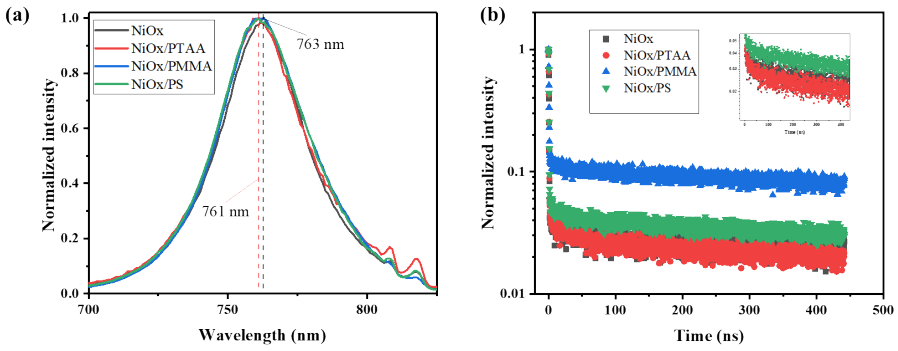

Figure S6. The steady-state PL (a) and time-resolved PL (b) for perovskite films on different substrates.

Table S1. Summary of perovskite solar cells based on NiOx with different NiOx modification methods.

Device Structures	*Voc* (V)	*Jsc* (mA cm^{-2})	*FF*	PCE (%)	Ref.
ITO/F6TCNNQ:NiOx/CsFAMA perovskite/PCBM/ZrAcac/Ag	1.12	23.18	0.80	20.86	1
FTO/Cs:NiOx /$MAPbI_3$/PCBM/ZrAcac/Ag	1.12	21.77	0.79	19.35	2
FTO/NiMgLiO/$MAPbI_3$/PCBM/ Ti(Nb)Ox/Ag	1.07	21.62	0.75	16.20	3
ITO/Cu:NiO/$CH_3NH_3PbI_3$/C_{60}/ BCP/Ag	1.12	22.28	0.81	20.26	4
ITO/NiOx/F2HCNQ/CsFAMAPbI_3/ PS/PCBM/Ag	1.14	23.44	0.83	22.10	5
FTO/N:NiOx/$CH_3NH_3PbI_3$/ PCBM/BCP/Ag	1.03	22.60	0.77	18.13	6
ITO/NiOx@KCl/CsFAMAPbI_3/ PCBM/ZrAcac/Ag	1.15	22.21	0.80	20.96	7
FTO/NiO/DEA/Perovskite/PCBM/ PN4N/Ag	0.95	20.90	0.80	15.90	8
ITO/NiOx@KCl @O_2 plasma /perovskite/PCBM/BCP/Ag	1.05	23.17	0.79	19.16	9
ITO/NiOx/NH_4F/Perovskite/ PCBM/BCP/Ag	1.09	22.45	0.77	18.94	10
ITO/ NiOx/m-NiOx/ CsFAMAPbI_xBr_{3-x}/PCBM/BCP/Ag	1.12	21.80	0.67	16.40	11
FTO/NiOx modified PEAI/$MAPbI_3$/PCBM/AgAl	1.09	24.27	0.77	20.31	12
ITO/NiOx/CsBr/$MA_{1-x}FA_x$ $PbI_{3-y}Cl_y$/PCBM/BCP/Ag	1.09	23.50	0.75	19.20	13
ITO/NiO/FDA/ $CH_3NH_3PbI_3$/PCBM/AgAl	NA	NA	NA	18.20	14
ITO/NiOx/4-bromobenzoic acid/$MAPbI_3$/PCBM/bis-C_{60}/Ag	1.11	21.70	0.76	18.40	15
ITO/NiOx/TPI-6MEO/$MAPbI_3$/PC BM/BCP/Ag	0.97	23.18	0.79	17.76	16
FTO/NiOx/PTAA/$FA_{1-x}MA_xPb$ $(I_{3-y}Br_y)$/PCBM/Au	1.06	21.54	0.75	17.10	17
FTO/NiOx/PS/$MAPbI_3$/PS/ PCBM/BCP/Ag	1.15	22.51	0.77	19.99	18

Works 1-6: doping method to improve conductivity, to tune energy level offset;

Works 7-18: surface treatment methods to improve interfacial contact (8, 10-14, 16-17), to tune energy level offset (9, 11, 15), to increase perovskite crystallization (7, 12-14, 16-18), to passivate defect state (12, 14, 16), to change surface wettability (15), to improve conductivity (14), to improve device stability (10, 12-16, 18).

Table S2. Influence of the polymer concentration on photovoltaic performance of the devices.

Substrates	Concentration (mg/mL)	*Voc* (V)	*FF* (%)	*Jsc* (mA cm^{-2})	PCE (%)
NiOx/PTAA	0.5	1.16	80.52	22.31	20.76
	1	1.19	81.71	22.23	21.56
	1.5	1.14	77.08	21.25	18.46
	2	1.11	74.19	17.92	14.71
NiOx/PMMA	0.5	1.16	78.05	22.43	20.39
	1	1.19	78.61	22.23	21.08
	1.5	1.14	74.78	20.95	17.86
	2	1.07	71.76	16.61	12.61
NiOx/PS	0.5	1.15	78.49	22.07	19.90
	1	1.17	79.47	22.38	20.84
	1.5	1.13	71.20	20.87	16.86
	2	1.07	62.02	18.17	12.06

Table S3. Forward and reverse *J-V* photovoltaic performance of PVSCs with different substrates under 1 sun illumination (100 mW cm^{-2}) (R means reverse and F is forward).

Substrate		*Voc* (V)	*FF* (%)	*Jsc* (mA cm^{-2})	PCE (%)	HI (%)
NiOx	R	1.12	78.82	21.77	19.23	1.03
	F	1.12	76.82	21.72	18.67	
NiOx/PTAA	R	1.19	81.71	22.23	21.56	1.05
	F	1.17	79.94	21.80	20.45	
NiOx/PMMA	R	1.19	78.61	22.23	21.08	1.10
	F	1.16	73.16	22.31	19.19	
NiOx/PS	R	1.17	79.47	22.38	20.84	1.04
	F	1.17	79.45	21.66	20.09	

Table S4. Detailed parameters extracted from Figure 2.

	Saturation dark current ($\times 10^{-4}$ mA cm^{-2})	Ideal factor	V_{TFL} (V)
NiOx	25.90	1.57	0.52
NiOx/PTAA	9.67	1.43	0.40
NiOx/PMMA	1.46	1.47	0.30
NiOx/PS	6.05	1.45	0.40

Table S5. Diffraction peak intensity and FWHM of the (110) peak in XRD patterns for the perovskite films on different substrates.

	NiOx	NiOx/PTAA	NiOx/PMMA	NiOx/PS
Intensity (count)	1036	1130	1188	1055
FWHM (°)	0.152	0.146	0.147	0.150

Table S6. The detailed life times for perovskite film on different substrates.

	t_1 (ns)	$Frac_1$ (%)	t_2 (ns)	$Frac_2$ (%)	t_{ave} (ns)
NiOx	0.46	21.34	165.45	78.66	130.24
NiOx/PTAA	0.47	31.50	124.44	68.50	85.39
NiOx/PMMA	0.51	6.42	291.04	93.58	272.39
NiOx/PS	0.46	24.38	193.36	75.62	146.33

Reference

[1] Chen W.; Zhou Y.; Wang L.; Wu Y.; Tu B.; Yu B.; Liu F.; Tam H. W.; Wang G.; Djurisic A. B.; Huang L.; He Z., Molecule-Doped Nickel Oxide: Verified Charge Transfer and Planar Inverted Mixed Cation Perovskite Solar Cell. *Adv. Mater.* **2018,** *30*, 1800515-1800523.

[2] Chen W.; Liu F.; Feng X.; Djurišić A. B.; Chan W. K.; He Z., Cesium Doped NiOx As an Efficient Hole Extraction Layer for Inverted Planar Perovskite Solar Cells. *Adv. Energy Mater.* **2017,** *7*, 1700722-1700729.

[3] Li G.; Jiang Y.; Deng S.; Tam A.; Xu P.; Wong M.; Kwok H. S., Overcoming the Limitations of Sputtered Nickel Oxide for High-Efficiency and Large-Area Perovskite Solar Cells. *Adv. Sci.* **2017,** *4*, 1700463.

[4] Chen W.; Wu Y.; Fan J.; Djurišić A. B.; Liu F.; Tam H. W.; Ng A.; Surya C.; Chan W. K.; Wang D.; He Z., Understanding the Doping Effect on NiO: Toward High-Performance Inverted Perovskite Solar Cells. *Adv. Energy Mater.* **2018,** *8*, 1703519-1703528.

[5] Ru P. B.; Bi E. B.; Zhang Y.; Wang Y. B.; Kong W. Y.; Sha Y. M.; Tang W. T.; Zhang P.; Wu Y. Z.; Chen W.; Yang X. D.; Chen H.; Han L. Y., High Electron Affinity Enables Fast Hole Extraction for Efficient Flexible Inverted Perovskite Solar Cells. *Adv. Energy Mater.* **2020,** *10*, 1903487-1903495.

[6] Zhou P.; Li B.; Fang Z.; Zhou W.; Zhang M.; Hu W.; Chen T.; Xiao Z.; Yang S., Nitrogen-Doped Nickel Oxide as Hole Transport Layer for High-Efficiency Inverted Planar Perovskite Solar Cells. *Solar RRL* **2019,** *3*, 1900164-1900171.

[7] Chen W.; Zhou Y.; Chen G.; Wu Y.; Tu B.; Liu F. Z.; Huang L.; Ng A. M. C.; Djurišić A. B.; He Z., Alkali Chlorides for the Suppression of the Interfacial Recombination in Inverted Planar Perovskite Solar Cells. *Adv. Energy Mater.* **2019,** *9*, 1803872-1803881.

[8] Bai Y.; Chen H. N.; Xiao S.; Xue Q. F.; Zhang T.; Zhu Z. L.; Li Q.; Hu C.; Yang Y.; Hu Z. C.; Huang F.; Wong K. S.; Yip H. L.; Yang S. H., Effects of a Molecular Monolayer Modification of NiO Nanocrystal Layer Surfaces on Perovskite Crystallization and Interface Contact toward Faster Hole Extraction and Higher Photovoltaic Performance. *Adv. Funct. Mater.* **2016,** *26*, 2950-2958.

[9] Zheng X.; Song Z.; Chen Z.; Bista S. S.; Gui P.; Shrestha N.; Chen C.; Li C.; Yin X.; Awni R. A.; Lei H.; Tao C.; Ellingson R. J.; Yan Y.; Fang G., Interface Modification of Sputtered NiOx As the Hole-Transporting layer for Efficient Inverted Planar Perovskite Solar Cells. *J. Mater. Chem. A* **2020,** *8*, 1972-1980.

[10] Wang S.; Zhu Y.; Wang C.; Ma R., NH4F as an Interfacial Modifier for High Performance NiOx-Based Inverted Perovskite Solar Cells. *Org. Electron.* **2020,** *78*, 105627-105633.

[11] Wang S.; Zhu Y.; Wang C.; Ma R., NH4F as an Interfacial Modifier for High Performance NiOx-Based Inverted Perovskite Solar Cells. *Org. Electron.* **2020,** *78*, 105627-105633.

[12] Liu Y.; Duan J.; Zhang J.; Huang S.; Ou-Yang W.; Bao Q.; Sun Z.; Chen X., High Efficiency and Stability of Inverted Perovskite Solar Cells Using Phenethyl Ammonium Iodide-Modified Interface of NiOx and Perovskite Layers. *ACS Appl. Mat. Interfaces* **2020,** *12*, 771-779.

[13] Zhang B.; Su J.; Guo X.; Zhou L.; Lin Z.; Feng L.; Zhang J.; Chang J.; Hao Y., NiO/Perovskite Heterojunction Contact Engineering for Highly Efficient and Stable Perovskite Solar Cells. *Adv. Sci.* **2020,** *7*, 1903044-1903053.

[14] Zhang J.; Luo H.; Xie W.; Lin X.; Hou X.; Zhou J.; Huang S.; Ou-Yang W.; Sun Z.; Chen X., Efficient and Ultraviolet Durable Planar Perovskite Solar Cells via a Ferrocenecarboxylic Acid Modified Nickel Oxide Hole Transport Layer. *Nanoscale* **2018,** *10*, 5617-5625.

[15] Wang Q.; Chueh C. C.; Zhao T.; Cheng J.; Eslamian M.; Choy W. C. H.; Jen A. K., Effects of Self-Assembled Monolayer Modification of Nickel Oxide Nanoparticles Layer on the Performance and Application of Inverted Perovskite Solar Cells. *ChemSusChem* **2017,** *10*, 3794-3803.

[16] Li Z.; Jo B. H.; Hwang S. J.; Kim T. H.; Somasundaram S.; Kamaraj E.; Bang J.; Ahn T. K.; Park S.; Park H. J., Bifacial Passivation of Organic Hole Transport Interlayer for NiOx-Based p-i-n Perovskite Solar Cells. *Adv. Sci.* **2019,** *6*, 1802163-1802171.

[17] Du Y.; Xin C.; Huang W.; Shi B.; Ding Y.; Wei C.; Zhao Y.; Li Y.; Zhang X., Polymeric Surface Modification of NiOx-Based Inverted Planar Perovskite Solar Cells with Enhanced Performance. *ACS Sustainable Chemistry & Engineering* **2018,** *6*, 16806-16812.

[18] Wang T.; Cheng Z. D.; Zhou Y. L.; Liu H.; Shen W. Z., Highly Efficient and Stable Perovskite Solar Cells via Bilateral Passivation Layers. *J. Mater. Chem. A* **2019,** *7*, 21730-21739.